Open Access Library Journal
2024, Volume 11, e12237
ISSN Online: 2333-9721
ISSN Print: 2333-9705

Theoretical Study on Electrical Properties of n-AlGaAs Schottky Barrier Diodes in a Diverse Temperature Range

Sonia Bouzgarrou[1,2*], Hanan Al-Shamari[1]

[1]Department of Physics, College of Science, Qassim University, Buraidah, Saudi Arabia
[2]Laboratoire de Microélectronique et Instrumentation (UR 03/13-04), Faculté des Sciences de Monastir, Monastir, Tunisia
Email: *b_sonia3@yahoo.fr

How to cite this paper: Bouzgarrou, S. and Al-Shamari, H. (2024) Theoretical Study on Electrical Properties of n-AlGaAs Schottky Barrier Diodes in a Diverse Temperature Range. *Open Access Library Journal*, **11**: e12237.
https://doi.org/10.4236/oalib.1112237

Received: September 4, 2024
Accepted: October 20, 2024
Published: October 23, 2024

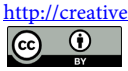

Abstract

In this paper, we report the study of I-V characteristics for some metal work functions. The Schottky barrier structure is controlled by the metal work function using the MATLAB programming language. The study of the effect of metal work function proved its influence on device performance, and a significant dependence was observed between this parameter and the electrical parameters at room temperature. The temperature effect on the electrical characteristics of n-AlGaAs Schottky diodes has been investigated at various temperatures ranging from 50 K to 500 K. Thermionic emission theory is used to determine the electrical parameters of a device. As a result of I-V characteristics, the ideality factor (n) decreased with increasing temperature, while the barrier height ($\varnothing_{b_n}$) increased. This strong dependence of Schottky diode parameters on temperature was attributed to the spatial inhomogeneity at the metal-semiconductor (MS) interface. By assuming a Gaussian distribution of the barrier heights at the MS interface, the inhomogeneity of the barrier height has been successfully explained. These results confirm the deviation of the TE current with decreasing temperature for Schottky diodes. These findings demonstrate that the n-AlGaAs structure exhibits a good diode and can be successfully applied in optoelectronic and photovoltaic applications.

Subject Areas

Applied Physics, Mathematics, Modern Physics

Keywords

Metal-Semiconductor Contacts, Thermionic Emission, Barrier Height, Electrical Behavior, Ideality Factor, Schottky Diodes

1. Introduction

Electron manipulation and storage are used in semiconductor electronics devices. Semiconductor devices operate on the basis of the basic principle that the conducting and optical properties of semiconductors can be altered easily and rapidly [1] [2]. One way this can be done is through the use of junctions between dissimilar materials. Junctions can form between N-type and P-type materials, between materials with different bandgaps, and between metals and semiconductors. The P-N junction is one of the most important junctions in solid-state electronics. The junction is used as a device in applications such as rectifiers, waveform shapers, variable capacitors, lasers, detectors, etc. These junctions also have special properties that are useful for devices. Metals by themselves are necessary to connect the semiconductors to the "outside world" of voltage sources and circuits [3]-[8]. They are also able to produce rectifying junctions. Insulators are also an integral part of electronics. These materials provide isolation between two regions of a device, can be used for band structure tailoring, can be used as capacitors, etc. In this research, we will examine some important properties of a variety of junctions.

Schottky diodes are unipolar devices, which means that only one type of carrier is available for current transport [9]-[12]. If they are designed for large blocking voltages, the resistance of the base will increase strongly due to the lack of charge carrier modulation, as will be shown in the following. Schottky power diodes have been used for a long time, but in the last few years, they have gained increased importance in the medium power range [13]-[15]. Schottky diodes are made from semiconductor materials with a wide bandgap. With these materials, much higher blocking voltages are possible due to the higher critical fields. However, since the increased bandgap leads to a comparatively high junction voltage in a bipolar device, a Schottky junction with a much smaller junction voltage has become an attractive alternative [16] [17].

In this work, we will study the electrical behavior and Schottky barrier height inhomogeneities of Schottky structures, by using classical model of *TE* current. First, the structure is studied for different metal work function ranged from 4.33 eV to 5.93 eV, at room temperature. Then, electrical parameters such as saturation current I_s, ideality factor (n), barrier height ($\varnothing_{b_n}$) are extracted from the current-voltage characteristics as a function of temperature. Electrical parameters are extracted for each temperature.

2. Simulation Setting

MATLAB, a computer software program, was used to simulate and discuss the contact AlGaAs structures and Schottky diode with n-doping. The modeled structure has a three-dimensional design. Once the structure has been defined, takes into account all the electrical and the optical properties. Among these attributes we mention mobility of electron μ_n, mobility of hole μ_p, dielectric constant, electronic affinity, the energy band gap, the effective state density in the conduction band and valence band, and so forth. The negligible density of donor and acceptor

states eliminates the impact of the interface states [18]. Furthermore, the impact of both temperature and work function on the electrical characteristics of the metal/n-AlGaAs Schottky structure was examined. The physical mechanisms of concentration-dependent mobility (CONMOB) [19] [20], Auger recombination rate (Auger) [21], and Shockley-Read-Hall (SRH) recombination [22] are modeled. In addition, the classical method is employed for the numerical solution operations.

3. Simulation and Results Outcomes

3.1. Aspects of the Physics of the Metal-Semiconductor Junction at Room Temperature

Metals form an important part of semiconductor technology. As shown in Figure 1, they are used as interconnects (*i.e.* low resistance conductors), they form Schottky barriers and Ohmic contacts, and they form gates in field effect transistors. The high density of mobile electrons, the resistivity of metals is very low.

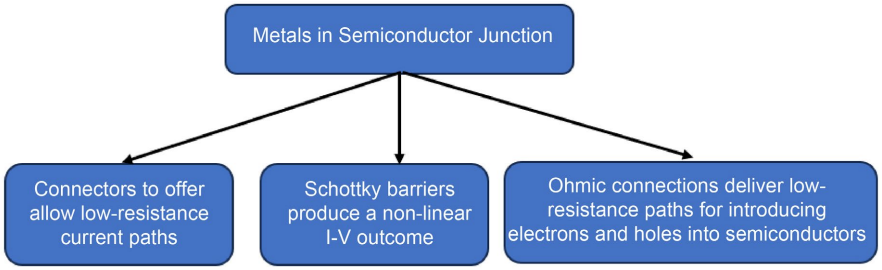

Figure 1. Metal used in semiconductor technology for three important applications.

In Table 1 we show the resistivities of some important metals used in electronics [18] [23]. In semiconductor circuits, interconnects provide pathways through which charge travels from one point to another. While these interconnects are obviously passive elements of the circuit, they are extremely important and play a role in circuit performance. The metal strips making up the interconnect must be able to carry adequate current and make good contact with the devices. Interconnects are deposited on insulators and touch the active devices only through windows that are opened at select points [24] [25].

Table 1. Some metals used in semiconductor devices and their resistivity's [18].

Materials	Resistivity (μΩ·cm)
Aluminum (Al)	
Bulk	2.7
Thin Film	0.2 - 0.3
Titanium (Ti)	40
Tungsten (W)	5.6
Ti-W	15 - 50

Continued

Gold (Au)	2.44
Silver (Ag)	1.59
Copper (Cu)	1.77
Platinum (Pt)	10
Silicide's	
PtSi	28 - 35
NiS_2	50

The metal-semiconductor junction can result in a junction that has non-linear diode characteristics similar to those of the P-N diode except that for many applications it has a much faster response since carrier transport is unipolar. Such a junction is called a Schottky barrier diode [26]-[28].

To understand the charge carrier transport across this junction we need to define some quantities relating the electron energies in the metal and semiconductor to the energy of a free electron, the so-called vacuum level:

$\varnothing_M$: work function for the metal

This is the energy, that must be added to an electron to allow it to escape from the metal, and this is equivalent to the difference between Fermi level, E_F, which is located in the conduction band of a metal and the vacuum level. In the semiconductor:

$\varnothing_S$: work function for the semiconductor

The work function for a semiconductor is also defined as the distance between the Fermi level and the vacuum level. However, the Fermi level of a non-degenerate semiconductor is positioned between the valence band and the conduction band and no electron is allowed to have this energy. Therefore, additionally we need to define:

χ : electron affinity for the semiconductor

This is the energy needed to remove an electron located at the bottom of the conduction band, E_C, where most of the conduction electrons reside, to the vacuum level outside the semiconductor.

The working of the Schottky diode depends upon how the metal-semiconductor junction behaves in response to external bias [29]. Let us pursue the approximation used for the P-N junction and examine the band profile of a metal and a semiconductor.

We will assume an ideal surface for the semiconductor in the first calculation. Later we will examine the effect of surface defects. If we assume that $\varnothing_M > \varnothing_S$ so that the Fermi level in the metal is at a lower position than in the semiconductor. This condition leads to an N-type Schottky barrier. When the junction between the two systems is formed, the Fermi levels should line up at the junction and remain flat in the absence of any current. At the junction, the vacuum energy

levels of the metal side and semiconductor side must be the same [30] [31].

To ensure the continuity of the vacuum level and align the Fermi levels. Electrons move out from the semiconductor side to the metal side. Note that since the metal side has an enormous electron density, the metal Fermi level or the band profile does not change when a small fraction of electrons are added or taken out. As electrons move to the metal side, they leave behind positively charged fixed dopants, and a dipole region is produced in the same way as for the P-N diode.

In the ideal Schottky barrier with no bandgap defect levels, the height of the barrier at the semiconductor-metal junction, is defined as the difference between the semiconductor conduction band at the junction and the metal Fermi level. This barrier is given by:

$$e\varnothing_b = e\varnothing_M - e\chi_S \tag{1}$$

The electrons coming from the semiconductor into the metal face a barrier denoted by eV_{bi}. The potential eV_{bi} is called the built-in potential of the junction and is given by:

$$eV_{bi} = -\left(e\varnothing_M - \varnothing_S\right) \tag{2}$$

It is possible to have a barrier for hole transport if $\varnothing_M < \varnothing_S$. In this case of a metal-P-type semiconductor junction where we choose a metal so that $\varnothing_M < \varnothing_S$. Therefore, at equilibrium the electrons are injected from the metal to the semiconductor, causing a negative charge on the semiconductor side. The bands are bent once again and a barrier is created for hole transport. The height of the barrier seen by the holes in the semiconductor is:

$$eV_{bi} = e\varnothing_S - e\varnothing_M \tag{3}$$

The values of work function of some metals are given in **Table 2** [2] [29] [32]. These values are approximate as they are very sensitive to surface impurities.

Table 2. Work function of some metals used.

Metal	Work function (ev)	References
Ag	4.26	[29]
	4.3	[1]
	4.7	[32]
Al	4.28	[29]
	4.3	[2]
Au	5.1	[32]
	4.8	[29]
Cr	4.5	[29]
	4.6	[32]
Ni	5.15	[29]
	4.4	[32]

Continued

Pt	5.65	[32]
	5.3	[29]
Cu	4.4	[29]
	4.65	[32]
	4.7	[2]
Fe	4.4	[32]
Mo	4.17	[2]
Ca	3.2	[32]
	3.0	[2]

The first section examines the impact of the metal work function on the electrical behavior at ambient temperature (300 K). The semi-log and linear current-voltage I-V characteristics of the metal/n-AlGaAs Schottky structure for some metal work functions are shown in Figure 2.

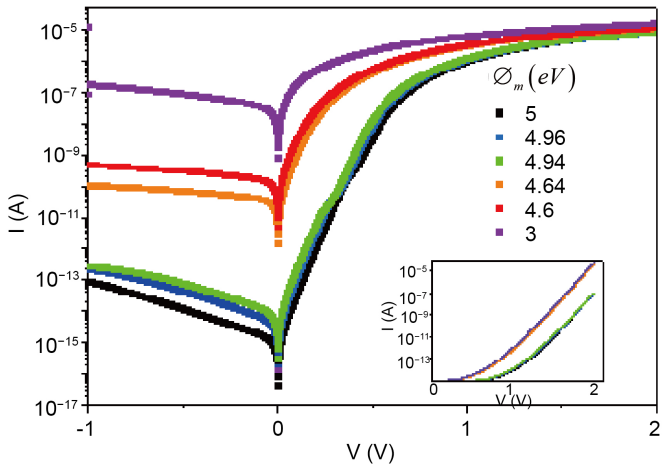

Figure 2. I-V characteristics of metal/n-AlGaAs for some metal work function at room temperature.

It is evident from the semi-log characteristics and reverse bias voltage that, for low metal work function, we get a significant reverse current that decreases as $\varnothing_M$ increases from 3.00 eV to 5.00 eV (Figure 2).

The Schottky characteristic behavior is observed under forward bias voltage for all values of $\varnothing_M$. At low bias voltages $V < 0.75$ V, the current increases linearly with bias voltage and subsequently drops as $\varnothing_M$ increases.

Furthermore, it is evident that for $\varnothing_M > 4.94$ eV, the plot has two separate linear regions with differing slopes, which correspond to Region II (at a bias region $0.35 < V \leq 0.75$ V) and Region I (low-bias region $V \leq 0.35$ V). This double barrier phenomenon can be explained as the emergence of an aberrant current under low forward bias. The current increases linearly with bias voltage and

gradually falls with rising $\varnothing_M$ for linear characteristics and forward bias voltage. Furthermore, it is noted that as $\varnothing_M$ grows, the threshold voltage V rises as well.

3.2. Thermionic Emission Theory

The thermionic emission is a phenomenon related to field emission. The thermionic emission is that the thermal energy given to charge carriers overcomes the binding potential, also known as work function of metals, such that electrons escape out from the surface of solid. The charge carrier can be electrons or ions. The basic theoretical model of thermionic emission is also based on Sommerfeld model of metal, the triangular vacuum potential barrier and the equilibrium electron emission [18]. The key point of the thermionic emission is that electrons in conduction band are driven to high excited states by heat such that the kinetic energy of electrons overcomes the vacuum potential barrier.

Besides, the diffusion and thermionic emission mechanisms, electrons can also be transported across the barrier by quantum mechanical tunneling.

The two ways in which tunneling can occur in a Schottky barrier junction are for both forward bias and reverse bias. The semiconductor is assumed to be doped to degeneracy such that the Fermi level lies above the bottom of the conduction band. Because of heavy doping, the depletion region is very thin, and at low temperatures, electrons with energy close to the Fermi level can tunnel from the semiconductor into the metal. This process is known as "field emission" (FE). At higher temperatures, a significant number of electrons are able to rise high above the Fermi level, where they see a thinner and lower barrier. These electrons can thus tunnel into the metal before reaching the top of the barrier. This tunneling of thermally excited electrons is known as "thermionic field emission" (TFE). Since the number of electrons decreases rapidly with energy above the Fermi level, and the barrier thickness and height also decrease, there exists an energy Em at which the contribution of TFE reaches its maximum. If the temperature is gradually raised still further, a limit is reached at which practically all the electrons are able to reach the top of the barrier, and thermionic emission predominates.

The rectifying characteristics of the Schottky junction can be described by an equation for the I-V characteristics, in analogy to related equation for the I-V characteristics of the PN-junction.

The current-voltage conduction classical model can be considered, by assuming that the TE theory is true in the current range for each temperature. For real Schottky contacts, the classical model of I-V characteristics is represented by this form [23] [33] [34]:

$$I = I_s\left[\exp\frac{V - R_s I}{nV_t} - 1\right] \tag{4}$$

where, $V_t = kT/q$

So,

$$I = I_s\left[\exp\frac{q\left(V - R_s I\right)}{nkT} - 1\right] \tag{5}$$

where n and R_s are the ideality factor and series resistance, respectively. q is the electron charge, k is the Boltzmann constant, V is the applied forward-bias voltage, T is the absolute temperature in kelvin. And I_s is the saturation current. Which can be defined as the following equation:

$$I_s = AA^*T^2 \exp\left(\frac{-q\varnothing_{b_n}}{kT}\right) \tag{6}$$

where A and A^* denote the contact diode area and the effective Richardson constant, respectively. $\varnothing_{b_n}$ represents the effective barrier height.

By taking into consideration that at the low bias voltage V, the current I is low, therefore the term R_sI is low compared to V, Equation (5) becomes:

$$I = I_s\left[\exp\frac{V}{nV_t} - 1\right] \tag{7}$$

By taking the logarithm of both sides

$$\ln(I) = \ln(I_s) + \ln\left(\exp\frac{V}{nV_t}\right) \tag{8}$$

Then, when we emplace V_t we obtained:

$$\ln(I) = \ln(I_s) + \frac{qV}{nkT} \tag{9}$$

This last equation is in the form of a line equation $y = ax + b$ with $b = \ln(I_s)$. To determine each parameter, we draw the graph $\ln(I)$ as a function of V from the equation of the line.

By taking the derivation of Equation (9) as a function of the voltage V, we can extract the ideality factor by:

$$\mathrm{d}\ln(I) = \frac{q}{nkT}\mathrm{d}V + \mathrm{d}\ln(I_s) \tag{10}$$

Since: $\mathrm{d}\ln(I_s) = 0$

$$\mathrm{d}\ln(I) = \frac{q}{nkT}\mathrm{d}V \tag{11}$$

We can extract n:

$$n = \frac{q}{kT}\frac{\mathrm{d}V}{\mathrm{d}\ln(I)} \tag{12}$$

where k is the Boltzmann constant, T is the temperature, and q is the electron charge. Here $\frac{\mathrm{d}V}{\mathrm{d}\ln(I)}$ is the slope of region 2.

The ideality factor (n) depends on the slope (a) of Equation (9) in the form of a straight line where: $y = ax + b$. From this equation we obtain:

$$a = \frac{q}{nkT} \tag{13}$$

which gives

$$n = \frac{q}{akT} \tag{14}$$

From the saturation current equation (Equation (6)), we can extract the barrier height. By taking the logarithm of both sides:

$$\ln\left(I_s\right) = \ln\left(AA^*T^2\right) + \frac{-q\varnothing_B}{kT} \tag{15}$$

$$\ln\left(AA^*T^2\right) - \ln\left(I_s\right) = \frac{q\varnothing_B}{kT} \tag{16}$$

where,

$$\ln\left(AA^*T^2\right) - \ln\left(I_s\right) = \ln\left(\frac{AA^*T^2}{I_s}\right) \tag{17}$$

By employing I_s values, the zero bias barrier height $\varnothing_{b_n}$ values are obtained from the following relation:

$$\varnothing_{b_n} = \frac{kT}{q}\ln\left(\frac{AA^*T^2}{I_s}\right) \tag{18}$$

For a fixed work function, I-V Characteristics of the Schottky contact on the linear scale and a semi-logarithmic scale simulated at different temperatures ranging from 50 K to 500 K are shown in Figure 3 and Figure 4, respectively.

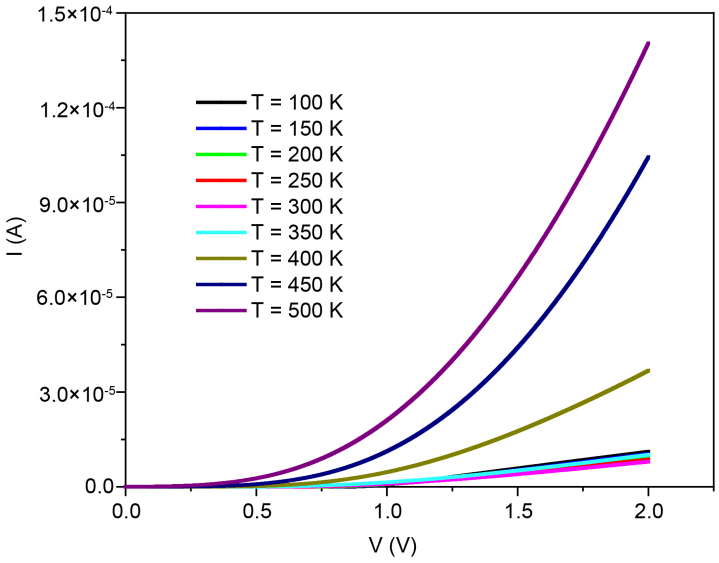

Figure 3. Linear forward bias I-V characteristics of metal/n-AlGaAs Schottky diode at different temperatures (100 K-500 K).

In low bias voltage ($V < 0.75$ V), the current rises rapidly with increasing bias voltage and varies linearly vs bias voltage. On the other hand, in high bias $V > 0.75$ V the current shows down enormously and varies also linearly with bias voltage and decreases gradually with decreasing temperature.

The value of the current at 50 K is very small due to the freezing phenomenon, where the mobility carriers are very low. Therefore, at 500 K the current increases

with increasing temperature. We see a significant leakage current which causes the influence of both temperature and barrier height on the saturation current. The reverse current increases with increasing reverse bias and no saturation are observed. This is a well-known defects-related phenomenon, for example surface state and or bulk defects [18] [34] [35].

The forward and reverse (I-V) characteristics of the Schottky diode on a semi-logarithmic scale measured at different temperatures ranging from 50 K to 500 K are shown in **Figure 4**. The diode has good rectifying behavior, as can be shown. Additionally, it is noted that when temperature rises, the linear region moves towards lower voltage values.

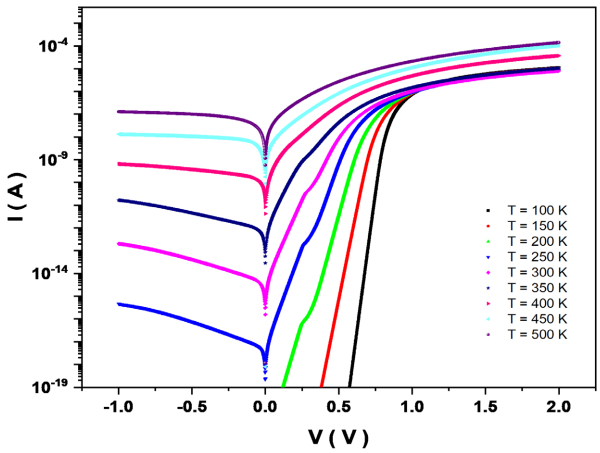

Figure 4. Semilogarithmic forward bias I-V characteristics of Metal/n-AlGaAs Schottky diode at different temperatures (100 K - 500 K).

The values of n, $\varnothing_{b_n}$, and I_s are obtained from Equations (6), (12), and (18). The linear region in the logarithmic (I-V) characteristics was used to derive these parameters. **Figure 5** shows the temperature dependence of the ideality factor n of structure. **Figure 6** shows the temperature dependence of the barrier height $\varnothing_{b_n}$ of structure. From **Figure 5**, the ideality factor n is decreased with increasing temperature. From **Figure 6**, the barrier height $\varnothing_{b_n}$ is increased with increasing temperature. For our structure, the values of n range from 3.16 at 50 K to 1.38 at 500 K. While the values of $\varnothing_{b_n}$ are ranged from 0.162 eV at 50 K to 1.073 at 500 K. These results are summarized in **Table 3**.

The conventional theory of TE theory that in an ideal situation, n should equal unity [35] [36]. However, a high value of n is found, indicating a departure from the hypothesis of TE. The breadth of the depletion region (Wd) and levels created by the interface states, which rely on the density of the doping atoms, may be the cause of these greater values of n at low temperatures [36]-[39]. This variation of the ideality factor n may be due to many factors. Such as generation–recombination effects, formation of barrier inhomogeneities… [40]-[43]

Moreover, **Figure 6** illustrates that while $\varnothing_{b_n}$ increases virtually exponentially. On the other hand, the value of n decreases with increasing temperature (**Figure**

5), following a double Gaussian distribution. The discrepancy seen in ideality factors and barrier height values implies that n-AlGaAs is not a perfect diode, and its charge transport mechanism is not limited to TE [18] [44]-[46].

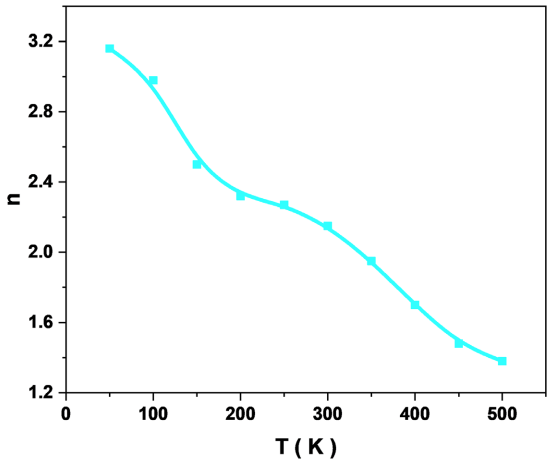

Figure 5. The temperature dependence of n of n-AlGaAs Schottky diode at a range of temperatures (50 K - 500 K).

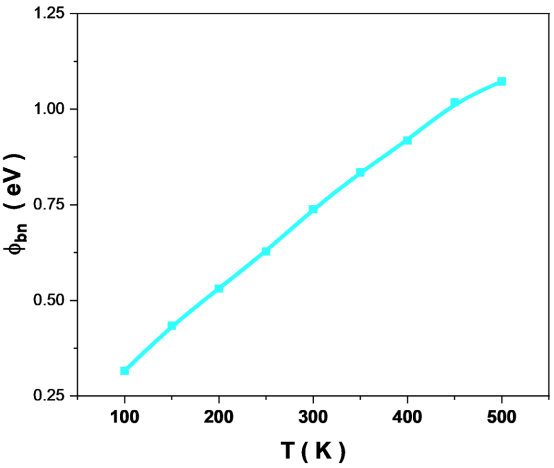

Figure 6. The temperature dependance of $\varnothing_{b_n}$ of n-AlGaAs Schottky diode at a range of temperatures (50 K - 500 K).

Table 3. The electrical parameters, in a range of 50 K to 500 K temperatures, calculated using Thermionic emission theory.

T (K)	Thermionic emission theory		
	N	$\varnothing_{b_n}$ (eV)	I_s (A)
50	3.16	0.162	2.26×10^{-14}
100	2.98	0.316	2.256×10^{-13}
150	2.5	0.434	1.15×10^{-11}
200	2.32	0.531	3.25×10^{-10}

Continued

250	2.27	0.628	2.55×10^{-9}
300	2.15	0.738	6.84×10^{-9}
350	1.95	0.835	2.25×10^{-9}
400	1.7	0.918	6.95×10^{-8}
450	1.48	1.018	1.55×10^{-7}
500	1.38	1.073	2.76×10^{-7}

4. Conclusion

A study of the current voltage (I-V) characteristics of Metal/n-AlGaAs Schottky diodes is investigated in wide temperature range 50 K to 500 K, using MATLAB programming language simulator. From the (I-V) characteristics, the electrical parameters are extracted using the thermionic emission theory. The ideality factor n is increased and the barrier height $\varnothing_{b_n}$ is decreased with decreasing temperature for our structure. The barrier height $\varnothing_{b_n}$ is exponentially distribution. On the other hand, the value of n decreases with increasing temperature, following a double Gaussian distribution.

Conflicts of Interest

The authors declare no conflicts of interest.

References

[1] Łukasiak, L. and Jakubowski, A. (2010) History of Semiconductors. *Journal of Telecommunications and Information Technology*, No. 1, 3-9. https://doi.org/10.26636/jtit.2010.1.1015

[2] Mesai, A.N., Lemkadem, I. and Benaouda, A. (2020) Etude de l'effet de temperature sur la diode Schottky. Master Thème, Université Echahid Hamma Lakhdar El-oued.

[3] Reddy Nallabala, N.K., Vattikuti, S.V.P., Verma, V.K., Singh, V.R., Alhammadi, S., Kummara, V.K., *et al.* (2022) Highly Sensitive and Cost-Effective Metal-Semiconductor-Metal Asymmetric Type Schottky Metallization Based Ultraviolet Photodetecting Sensors Fabricated on N-Type GaN. *Materials Science in Semiconductor Processing*, **138**, Article 106297. https://doi.org/10.1016/j.mssp.2021.106297

[4] Ulusoy, M., Badali, Y., Pirgholi-Givi, G., Azizian-Kalandaragh, Y. and Altındal, Ş. (2023) The Capacitance/Conductance and Surface State Intensity Characteristics of the Schottky Structures with Ruthenium Dioxide-Doped Organic Polymer Interface. *Synthetic Metals*, **292**, Article 117243. https://doi.org/10.1016/j.synthmet.2022.117243

[5] Kocyigit, A., Yilmaz, M., Aydogan, S., İncekara, Ü. and Kacus, H. (2021) Comparison of N and P Type Si-Based Schottky Photodiode with Interlayered Congo Red Dye. *Materials Science in Semiconductor Processing*, **135**, Article 106045. https://doi.org/10.1016/j.mssp.2021.106045

[6] Bouzgarrou, S., Ben Salem, M.M., Hassen, F., Kalboussi, A. and Souifi, A. (2005) DLTS and PL Study of Defects in InALAs/InP Heterojunctions Grown by Metal Organic Chemical Vapor Deposition. *Materials Science and Engineering: B*, **116**, 202-207. https://doi.org/10.1016/j.mseb.2004.10.007

[7] Ben Salem, M.M., Bouzgarrou, S., Sghaier, N., Kalboussi, A. and Souifi, A. (2006) Correlation between Static Characteristics and Deep Levels in InALAs/InGaAs/InP HEMT'S. *Materials Science and Engineering*: *B*, **127**, 34-40. https://doi.org/10.1016/j.mseb.2005.09.047

[8] Bouzgarrou, S., Sghaier, N., Ben Salem, M.M., Souifi, A. and Kalboussi, A. (2008) Influence of Interface States and Deep Levels on Output Characteristics of InALAs/InGaAs/InP Hemts. *Materials Science and Engineering: C*, **28**, 676-679. https://doi.org/10.1016/j.msec.2007.10.075

[9] Bouzgarrou, S. (2013) Experimental and Theoretical Study of Parasitic Effects in InALAs/InGaAs/InP HEMT'S. *American Journal of Physics and Applications*, **1**, 18-24. https://doi.org/10.11648/j.ajpa.20130101.14

[10] Türüt, A. (2020) Oncurrent-Voltage and Capacitance-Voltage Characteristics of Metal-Semiconductor Contacts. *Turkish Journal of Physics*, **44**, 302-347. https://doi.org/10.3906/fiz-2007-11

[11] Asubay, S., Güllü, Ö. and Türüt, A. (2009) Determination of the Laterally Homogeneous Barrier Height of Metal/*p*-InP Schottky Barrier Diodes. *Vacuum*, **83**, 1470-1474. https://doi.org/10.1016/j.vacuum.2009.06.050

[12] Sadoun, A. (2020) Extraction of the Electrical Parameters of the Au/InSb/InP Schottky Diode in the Temperature Range (300 K-425 K). *International Journal of Energetica*, **5**, 31-37. https://doi.org/10.47238/ijeca.v5i1.120

[13] Yıldız, D.E., Karadeniz, S., Yıldırım, M., Tasaltın, N., Gulsaran, A., Bastug Azer, B., *et al.* (2024) Novel PANI: Borophene/Si Schottky Device for the Sensitive Detection of Illumination and NaCl Salt Solutions. *Journal of Materials Science: Materials in Electronics*, **35**, Article No. 469. https://doi.org/10.1007/s10854-024-12243-x

[14] Koksal, N.E., Sbeta, M., Atilgan, A. and Yildiz, A. (2021) Al-Ga Co-Doped ZnO/Si Heterojunction Diodes. *Physica B*: *Condensed Matter*, **600**, Article 412599. https://doi.org/10.1016/j.physb.2020.412599

[15] Demirezen, S., Arslan Alsaç, A., Çetinkaya, H.G. and Altındal, Ş. (2023) The Investigation of Current-Transport Mechanisms (CTMs) in the Al/(In_2S_3: PVA)/*p*-Si (MPS)-Type Schottky Barrier Diodes (SBDs) at Low and Intermediate Temperatures. *Journal of Materials Science: Materials in Electronics*, **34**, Article No. 1186. https://doi.org/10.1007/s10854-023-10592-7

[16] Buyukbas-Ulusan, A., Tataroglu, A. and Altındal-Yerişkin, S. (2023) Analysis of the Current Transport Characteristics (CTCs) in the Au/n-Si Schottky Diodes (SDs) with Al_2O_3 Interfacial Layer over Wide Temperature Range. *ECS Journal of Solid State Science and Technology*, **12**, Article 083010. https://doi.org/10.1149/2162-8777/acf06e

[17] Choi, H., Jeon, J.D., Kim, S.E., Jang, S.Y., Sung, J.Y. and Lee, S.W. (2023) Strained $BaTiO_3$ Thin Films via *in-situ* Crystallization Using Atomic Layer Deposition on $SrTiO_3$ Substrate. *Materials Science in Semiconductor Processing*, **160**, Article 107442. https://doi.org/10.1016/j.mssp.2023.107442

[18] Sze, S.M. (1981) Physics of Semiconductor Devices. 2nd Edition, Wiley.

[19] Caughey, D.M. and Thomas, R.E. (1967) Carrier Mobilities in Silicon Empirically Related to Doping and Field. *Proceedings of the IEEE*, **55**, 2192-2193. https://doi.org/10.1109/proc.1967.6123

[20] Selberherr, S. (1984) Process and Device Modeling for Visi. *Microelectronics Reliability*, **24**, 225-257. https://doi.org/10.1016/0026-2714(84)90450-5

[21] Selberherr, S. (2012) Analysis and Simulation of Semiconductor Devices. Springer

Science & Business Media.

[22] Shockley, W. and Read, W.T. (1952) Statistics of the Recombinations of Holes and Electrons. *Physical Review*, **87**, 835-842. https://doi.org/10.1103/physrev.87.835

[23] Schroder, D.K. (2005) Semiconductor Material and Device Characterization. Wiley. https://doi.org/10.1002/0471749095

[24] Hudait, M.K. and Krupanidhi, S.B. (2000) Effects of Thin Oxide in Metal-Semiconductor and Metal-Insulator-Semiconductor Epi-GaAs Schottky Diodes. *Solid-State Electronics*, **44**, 1089-1097. https://doi.org/10.1016/s0038-1101(99)00320-2

[25] Chattopadhyay, P. (1994) Effect of Localized States on the Current-Voltage Characteristics of Metal-Semiconductor Contacts with Thin Interfacial Layer. *Solid-State Electronics*, **37**, 1759-1762. https://doi.org/10.1016/0038-1101(94)90223-2

[26] Güllü, Ö. and Türüt, A. (2010) Electrical Analysis of Organic Dye-Based MIS Schottky Contacts. *Microelectronic Engineering*, **87**, 2482-2487. https://doi.org/10.1016/j.mee.2010.05.004

[27] Tataroğlu, A., Altındal, Ş. and Azizian-Kalandaragh, Y. (2020) Comparison of Electrical Properties of MS and MPS Type Diode in Respect of (In_2O_3-PVP) Interlayer. *Physica B*: *Condensed Matter*, **576**, Article 411733. https://doi.org/10.1016/j.physb.2019.411733

[28] Alptekin, S., Tan, S.O. and Altindal, S. (2019) Determination of Surface States Energy Density Distributions and Relaxation Times for a Metal-Polymer-Semiconductor Structure. *IEEE Transactions on Nanotechnology*, **18**, 1196-1199. https://doi.org/10.1109/tnano.2019.2952081

[29] Stössel, M., Staudigel, J., Steuber, F., Simmerer, J. and Winnacker, A. (1999) Impact of the Cathode Metal Work Function on the Performance of Vacuum-Deposited Organic Light Emitting-Devices. *Applied Physics A*: *Materials Science & Processing*, **68**, 387-390. https://doi.org/10.1007/s003390050910

[30] Vick, A.J. (2011) Measuring Low Dimensional Schottky Barriers of Rare Earth Silicide-Silicon Interfaces. PhD Thesis, University of York.

[31] Ghods, A. (2020) Design and Fabrication of Field-Effect III-V Schottky Junction Solar Cells. Doctoral Dissertations, Missouri University of Science and Technology.

[32] Helal, H., Benamara, Z., Kacha, A.H., Amrani, M., Rabehi, A., Akkal, B., *et al.* (2019) Comparative Study of Ionic Bombardment and Heat Treatment on the Electrical Behavior of Au/GaN/n-GaAs Schottky Diodes. *Superlattices and Microstructures*, **135**, Article 106276. https://doi.org/10.1016/j.spmi.2019.106276

[33] Hou, L., Hou, Y., Zhu, M., Tang, J., Liu, J., Wang, H., *et al.* (2005) Formation and Transformation of $ZnTiO_3$ Prepared by Sol-Gel Process. *Materials Letters*, **59**, 197-200. https://doi.org/10.1016/j.matlet.2004.07.046

[34] Barkhordari, A., Özçelik, S., Pirgholi-Givi, G., Mashayekhi, H.R., Altındal, Ş. and Azizian-Kalandaragh, Y. (2021) Dielectric Properties of PVP: $BaTiO_3$ Interlayer in the Al/PVP: $BaTiO_3$/P-Si Structure. *Silicon*, **14**, 5437-5443. https://doi.org/10.1007/s12633-021-01196-z

[35] Reddy, P.R.S., Janardhanam, V., Shim, K., Reddy, V.R., Lee, S., Park, S., *et al.* (2020) Temperature-Dependent Schottky Barrier Parameters of Ni/Au on N-Type (001) β-Ga_2O_3 Schottky Barrier Diode. *Vacuum*, **171**, Article 109012. https://doi.org/10.1016/j.vacuum.2019.109012

[36] Kim, D.M., Kim, D.H. and Lee, S.Y. (2007) Characterization and Modeling of Temperature-Dependent Barrier Heights and Ideality Factors in GaAs Schottky Diodes. *Solid-State Electronics*, **51**, 865-869. https://doi.org/10.1016/j.sse.2007.04.006

[37] Barkhordari, A., Mashayekhi, H.R., Amiri, P., Altındal, Ş. and Azizian-Kalandaragh, Y. (2024) Optoelectric Response of Schottky Photodiode with a PVP: $ZnTiO_3$ Nanocomposite as an Interfacial Layer. *Optical Materials*, **148**, Article 114787. https://doi.org/10.1016/j.optmat.2023.114787

[38] Nawar, A.M., Abd-Elsalam, M., El-Mahalawy, A.M. and El-Nahass, M.M. (2020) Analyzed Electrical Performance and Induced Interface Passivation of Fabricated Al/NTCDA/P-Si MIS-Schottky Heterojunction. *Applied Physics A*, **126**, Article No. 113. https://doi.org/10.1007/s00339-020-3289-y

[39] Demirezen, S. (2019) The Role of Interface Traps, Series Resistance and (Ni-Doped PVA) Interlayer Effects on Electrical Characteristics in Al/p-Si (MS) Structures. *Journal of Materials Science*: *Materials in Electronics*, **30**, 19854-19861. https://doi.org/10.1007/s10854-019-02352-3

[40] Çiçek, O., Tecimer, H.U., Tan, S.O., Tecimer, H., Altındal, Ş. and Uslu, İ. (2016) Evaluation of Electrical and Photovoltaic Behaviours as Comparative of Au/N-GaAs (MS) Diodes with and without Pure and Graphene (Gr)-Doped Polyvinyl Alcohol (PVA) Interfacial Layer under Dark and Illuminated Conditions. *Composites Part B*: *Engineering*, **98**, 260-268. https://doi.org/10.1016/j.compositesb.2016.05.042

[41] Elamen, H., Badali, Y., Ulusoy, M., Azizian-Kalandaragh, Y., Altındal, Ş. and Güneşer, M.T. (2023) The Photoresponse Behavior of a Schottky Structure with a Transition Metal Oxide-Doped Organic Polymer (RuO_2: PVC) Interface. *Polymer Bulletin*, **81**, 403-422. https://doi.org/10.1007/s00289-023-04725-5

[42] Werner, J.H. and Güttler, H.H. (1991) Barrier Inhomogeneities at Schottky Contacts. *Journal of Applied Physics*, **69**, 1522-1533. https://doi.org/10.1063/1.347243

[43] Marnadu, R., Chandrasekaran, J., Vivek, P., Balasubramani, V. and Maruthamuthu, S. (2019) Impact of Phase Transformation in WO_3 Thin Films at Higher Temperature and Its Compelling Interfacial Role in Cu/WO_3/p-Si Structured Schottky Barrier Diodes. *Zeitschrift für Physikalische Chemie*, **234**, 355-379. https://doi.org/10.1515/zpch-2018-1289

[44] Badali, Y., Altan, H. and Altındal, S. (2024) Thermal Dependence on Electrical Characteristics of Au/(PVC: Sm_2O_3)/n-Si Structure. *Journal of Materials Science: Materials in Electronics*, **35**, Article No. 228. https://doi.org/10.1007/s10854-023-11898-2

[45] Demirezen, S., Ulusoy, M., Durmuş, H., Cavusoglu, H., Yılmaz, K. and Altındal, Ş. (2023) Electrical and Photodetector Characteristics of Schottky Structures Interlaid with P(EHA) and P(EHA-*co*-AA) Functional Polymers by the iCVD Method. *ACS Omega*, **8**, 46499-46512. https://doi.org/10.1021/acsomega.3c04935

[46] Taşçıoğlu, İ., Pirgholi-Givi, G., Yerişkin, S.A. and Azizian-Kalandaragh, Y. (2023) Examination on the Current Conduction Mechanisms of Au/n-Si Diodes with ZnO-PVP and ZnO/Ag_2WO_4-PVP Interfacial Layers. *Journal of Sol-Gel Science and Technology*, **107**, 536-547. https://doi.org/10.1007/s10971-023-06177-9